The International Journal of Materials and Engineering Technology (TIJMET) (2022) 5(1)
http://dergipark.gov.tr/tijmet
ISSN: 2667-4033

RESEARCH ARTICLE

Analysis of mechanical behavior of thermoplastic composites

Ali Taner Kuzu[1], Elifnur Kosemen[2], Aysu Hande Yucel[*2], Mustafa Bakkal[2]

[1]*Isik University, Department of Mechanical Engineering, Istanbul, Turkey*
[2]*Istanbul Technical University, Department of Mechanical Engineering, Istanbul, Turkey*

Article Info

Article history:
Received 19.11.2021
Revised: 16.01.2022
Accepted: 31.01.2022
Published Online: 04.03.2022

Keywords:
Composites
Mechanical testing
Thermoplastic matrix

Abstract

This paper presents the effect of fiber orientation on the tensile, compression, impact, and flexural properties of glass fiber reinforced acrylic-based thermoplastic composites. The mechanical behavior of three different composite plates, produced by the resin transfer molding (RTM) method, with 0°/90°/45°, 0°/90° and ±45° glass fiber orientations were investigated by carrying out tensile, compression, three-point bending and Charpy impact tests. A Weibull distribution model was implemented to explain the variation in mechanical properties of the acrylic-based composite. According to Weibull analysis results with 63.2% probability, the highest tensile strength (561 MPa), compressive strength (293 MPa) and impact values (19.44 J) were obtained when the plate with 0°/90° glass fiber orientation was tested, whereas the highest flexural strength was obtained when the plate with 0°/90°/45° was tested.

1. Introduction

Glass fiber reinforced polymer materials (GFRP) have become an important focus of interest in industry due to their low density, low thermal expansion, moderate stiffness and high strength [1]. The manufacturing parameters of these materials; the fiber orientation, the type of fiber and resin, the production temperature of the composite components play a major role in enhancing mechanical strength [2-4]. Thanks to the advantage of managing the mechanical properties of the final product by changing the above-mentioned parameters, especially changing fiber orientation, these materials have started to be used extensively in industry. Therefore, the correlation between fiber orientation and providing the desired mechanical properties from the composite is critical for the design and application of composite structures.

In recent years, interest in recyclable and low-weight materials has increased especially in the automotive industry. Concordantly, there has been increasing research effort and specialization in the development of thermoplastic composites that provide high specific strength and recyclable properties. However, the use of thermoplastic composites has been limited due to their complex preparation and manufacturing processes [5]. The use of thermoplastics as matrix materials in composites is 25%-35%, among which the most common materials are Polypropylene (PP), Polyethylene (PE), and polyetherimide (PEI) [6]. Thermoplastic materials require both high processing temperatures and expensive equipment for composite production [7]. A novel acrylic-based thermoplastic, recently introduced by Arkema is Elium® [8, 9]. This is becoming a popular matrix material as its ability to polymerize at room temperature provides a great advantage over other thermoplastic matrix materials [10, 11]. Acrylic-based thermoplastic matrix materials also enhance the impact and fracture toughness properties of the composite structure [9, 12].

A number of studies have been undertaken to explore the effect of fiber directions on mechanical properties. However, there is not a large body of work in this area which consider thermoplastic matrix materials, especially for acrylic-based thermoplastics. Kinvi-Dossou et al. compared the mechanical behavior under impact loading of acrylic thermoplastic composites versus conventional GFRP which has a thermoset matrix and found that the acrylic thermoplastic composite outperformed the traditional GFRP [13]. Kazemi et al. investigated the mechanical properties of hybrid fiber reinforced polymer composites with acrylic thermoplastic composites. Tensile, compression, and shear test results found that the mechanical properties of acrylic thermoplastic composites are comparable to thermoset-based composites [14]. Similar work has also been pursued by Obande et al. who conducted research to benchmark the mechanical performance of glass fiber-reinforced thermoplastic acrylic matrices against thermosetting epoxy laminates produced by vacuum-assisted resin transfer molding. The acrylic composite exhibited superior tensile (90°), flexural (0°), interlaminar shear, and fracture toughness properties [15]. With the exception of the study reported by Cousins [16], tensile, compression, bending, and shearing properties of acrylic and comparable epoxy composites have not been thoroughly examined.

The goal of this paper is to determine the mechanical properties of thermoplastic composites produced with ±45°, 0°/90°, and 0°/90°/45° orientations. It is aimed to compare acrylic-based thermoplastic composites with conventional thermoset composites, whose mechanical properties have been determined and reported in this paper, to determine whether these composites are materials that can match the mechanical properties of thermoset composites.

Corresponding Author: Aysu Hande Yucel
E-mail: ayesilova@itu.edu.tr

How to cite this article:
Kuzu, A.T., Kosemen, E., Yucel, A.H., Bakkal, M., Analysis of mechanical behavior of thermoplastic composites, The International Journal of Materials and Engineering Technology (TIJMET), 2022, 5(1): 7-12

2. Materials and methods

2.1. The composite material production process

In this study, composite plates with 0°/90°/45°, 0°/90° and ±45° glass fiber orientations were produced using RTM method. At the beginning of production, the tool surface was heated to 25°C. By setting the necessary safety and cleaning conditions for the start of the process, 5 layers of Marbocote 277-CEE release agent were applied with lint-free wipes, with 15 minutes between each application. After waiting for one hour for the final coating to fully cure, the glass fiber layers were cut to the required dimensions (490 x 490 mm), laid up in the desired fibre orientation and then weighed to record the mass of the dry fabric. Ensuring that no glass fiber overhangs the resin gateway, glass fiber was loaded into the tool cavity. The mould tool was closed, and vacuum pressure was applied to the mould cavity and flange. It was ensured that the vacuum level was <20 mbar and that there were no air leaks. The injection machine was set to recirculate the resin and catalyst and it was checked that the catalyst mix percentage was set at 1.5 wt.% and that there were no bubbles or leaks. After the parameters of injection pressure (0.3 bar), injection start speed (15%) and injection speed (25%) were programmed in the injection machine setup, the injection was started. The injection was stopped when the resin reached the vacuum outlet. The resin system was left to cure for 2 hours at 25°C. When curing was finished, the composite plate was removed from the mold. The cured plate was post-cured at 80°C for four hours in the oven. The resin flash was cut off the edges of the plate and the plate mass was recorded. The composition and the properties of the glass fiber and matrix resin in GFRP plates are given in Table 1 for three different fiber orientations.

Experimental samples were obtained by cutting the plates to the appropriate dimensions using a water jet cutter according to the standards of the tests to be performed. The dimensions of the test samples are given in Table 2.

2.2. Test procedures

The tensile tests, compressive tests and three-point bending tests were conducted using the Shimadzu 50 kN testing machine. The deformation speed of the tensile and compressive tests was chosen as 2 mm/min in accordance with ASTM D3039/D3039M and ISO 14126:1999 standards. The deformation speed of the three-point bending test was chosen as 1 mm/min in accordance with ASTM D7264/D7264M standard. ASTM D7136/D7136M standard was used as a guide in impact tests that were completed with Charpy impact testing machine for measuring the damage resistance of a fiber-reinforced polymer matrix composite. All tests were continued until damage occurred in the sample. The tensile, compressive, three-point bending and impact test setups are shown in Figure 1a, 1b, 1c and 1d.

Table 1. Properties of composite plates.

Orientation	Fiber weight [%]	Fabric type	Matrix	# of layers	Hardener
0°/90°/45°	0.54-0.57	curl fabric	Elium® 151S	8	1.5% Nuvocure
±45°	0.54-0.57	curl fabric	Elium® 151S	8	1.5% Nuvocure
0°/90°	0.54-0.57	curl fabric	Elium® 151S	8	1.5% Nuvocure

Table 2. Dimensions and number of glass fiber reinforced composite test plates.

Test type	Specimen dimensions [mmxmmxmm]	Number of each specimen according to the fiber orientations		
		0°/90°	± 45°	0/90°/±45°
Tensile testing	250x25x4	10	10	10
Impact testing	160x13x4	10	10	10
Flexural testing	160x13x4	10	10	10
Compression testing	140x13x4	10	10	10

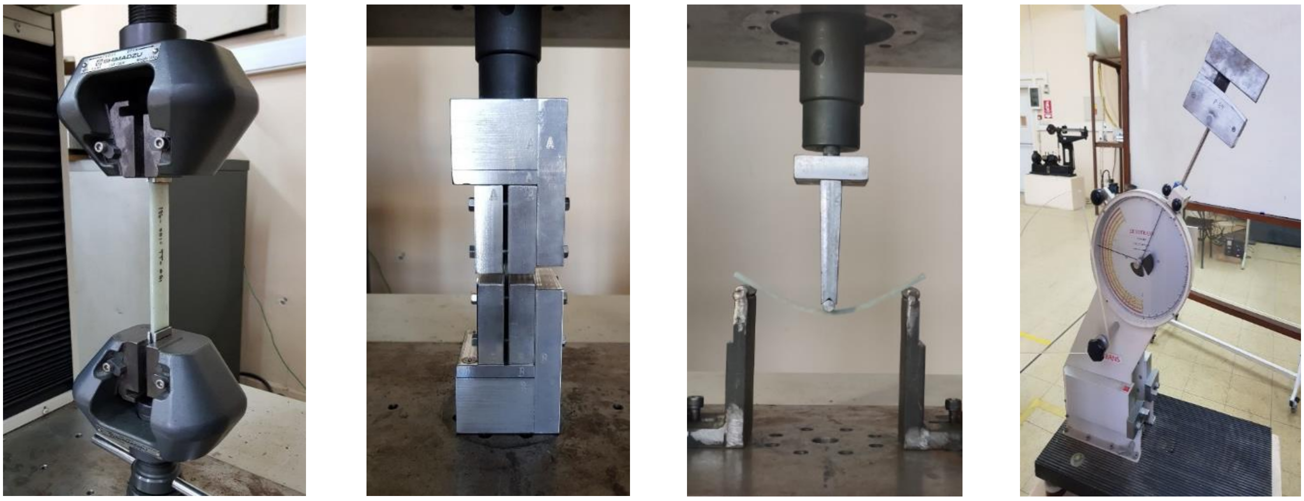

(a) (b) (c) (d)

Figure 1. (a) Tensile test setup, (b) compressive test setup, (c) three-point bending test setup and (d) impact test setup.

2.3. Statistical analysis of results

The probability distribution with the most common use in reliability studies is the Weibull distribution that offers a flexible reliability model as it can be used in all situations where the error rate is increasing, decreasing and constant [17]. The two-parameter Weibull distribution function is given by:

$$P_{r_k}=F(\sigma)=1-e^{\left[-\frac{\sigma}{\sigma_0}\right]^m} \quad (1)$$

where Prk, or F is the probability value for specific σ, m is the shape parameter or Weibull modulus, and "σ" _"0" is the scale parameter of the distribution. The Weibull modulus, m, is related to the distribution of data. The higher the value of m, which is the most important parameter of distribution, the lower the distribution of data. The mean estimated data which can be ultimate tensile stress for the tensile test is related to the scale parameter.

In this statistical method, the parameters of the Weibull probability distribution are determined by plotting. In the graphic method, the data is first sorted from small to large and row squares are calculated for each observation value. Eq. 2 is used to calculate the median of rank.

$$P_{r_k}=F(\sigma)=\frac{i-0.3}{N+0.4}\times 100 \quad (2)$$

The i and N terms can be introduced by the number of data rows and the total sample size. After the row squares of the data are determined, data and row medians are plotted on the graph. The graph contains test results on the x-axis and cumulative probability percentages on they y-axis. Among these points, the most possible line is obtained. This directly obtained value is the estimated value of the shape parameter. When the value on the line drawn parallel to the x-axis is drawn from a vertical line from F (σ), the point where the line intersects the x-axis is the value of the scale parameter. After the parameters have been calculated, certain time values can be predicted from the Weibull reliability function. The Weibull probability plot of the distribution begins with the transformation expressed as Eq. 3.

$$\ln\left(\ln\frac{1}{1-P_{r_k}}\right)=m\times\ln\sigma-m\times\ln\sigma_0 \quad (3)$$

The graph is a straight line (y=a×x+b) for the two-parameter distribution, while the graph is a curve in the three-parameter distribution. In the graphical method, after the data is sorted from small to large, $x_i=\ln(\sigma_i)$ and $y_i=\ln\left(\ln\frac{1}{1-P_{r_k(i)}}\right)$ are calculated. Thus, a graph is drawn with these values [12].

In this study, experimental results were analyzed with Weibull distribution and the results were analyzed statistically. In the experiments, the failure probabilities of the samples were calculated by Equation 2. The term P_{rk} is used here to describe the probability of failure. σ and σ_0 denote applied stresses and characteristic stresses respectively. Graphs created with $x_i=\ln(\sigma_i)$ and $y_i=\ln\left(\ln\frac{1}{1-Pr_k}\right)$ as a result of experimental data are linear lines. In points where these linear lines intersect 0 on the y-axis, the probability is given in Eq. 4.

$$Pr_k=1-\frac{1}{e}=0.632=63.2\% \quad (4)$$

The reliability of the experimental data was statistically analyzed according to the point where the curves intersect 0 on the y-axis.

3. Results and discussion

3.1. Tensile test

The results of the tensile test are given in Table 3. In plates with ±45° orientation, a linear elastic elongation first occurred and then the strength of the sample decreased slightly. Up to this point, the deformation behavior of GFRP with ±45° orientation resembles the typical stress-strain curve of thermoplastic materials. In the continuation of the test, as seen in thermoplastic composites, the strength slightly increased due to the effect of ±45° fiber reinforcements and subsequently rupture occurred. Unlike GFRP with ±45° orientation, linear elastic behavior was observed up to the break point in plates with 0°/90° and 0°/90°/45° orientations. The strength of the plates with 0°/90° orientation (547 ± 31 MPa) was measured higher than the strength of plates with 0°/90°/45° orientation (407 ± 34 MPa) because this plate has a higher amount of fiber which carries the tensile load in the deformation direction. The maximum strain before the break is attributed to the higher density of brittle fibers in the tensile direction for plates with 0°/90° and 0°/90°/45° orientations.

Table 3. Results of glass fiber reinforced composite test plates according to tensile tests.

Orientation	Modulus of elasticity [MPa]	UTS [MPa]	ε_{break} [mm/mm]	$\varepsilon_{\sigma_{max}}$ [mm/mm]
0°/90°/45°	6943 ± 404	407 ± 34	6 ± 0.50	6 ± 0.50
0°/90°	8378 ± 619	547 ± 31	6.75 ± 0.54	6.75 ± 0.55
± 45°	2851 ± 362	186 ± 11	23 ± 2.80	21 ± 2.80

3.2. Compression test

In plates with ±45° orientation (120 ± 6 MPa), the compressive strength first increased slowly and then the same strength was observed for a certain period of time. As shown in Table 4, the maximum strain before the break is attributed to the lower density of brittle fibers in the compression direction for the plate with ±45° orientation. Compression tests of plates with 0°/90°/45° and 0°/90° orientation showed a similar stress-strain curve and their strength was measured as 262 ± 23 MPa and 282 ± 21 MPa, respectively. In these plates, the compressive strength slowly increased linearly, then sudden damage occurred.

Table 4. Results of glass fiber reinforced composite test plates according to compression tests.

Orientation	Modulus of Elasticity [MPa]	UTS [MPa]	ε_{break} [%]	$\varepsilon_{\sigma_{max}}$ [%]
0°/90°/45°	744 ± 56	262 ± 23	47 ± 5	47 ± 5
0°/90°	924 ± 31	282 ± 21	42 ± 4	42 ± 4
±45°	332 ± 50	120 ± 6	96 ± 11	77 ± 12

3.3. Three-point bending test

In the plate with ±45° orientation, the damage occurred at a much lower value than plates with 0°/90° and 0°/90°/45° orientations as can be seen in Table 5. In addition to this, the strain at the point of maximum stress of the plate with ±45° orientation was measured higher than other orientations' strain at this point. Stress-strain curve behavior of the three-point bending test of plates with 0°/90° and 0°/90°/45° orientations was observed similarly, and the plate with 0°/90° orientation had higher flexural strength than the plate with 0°/90°/45° orientation.

Table 5. Results of glass fiber reinforced composite test plates according to three-point bending tests.

Orientation	E_f^{chord} [GPa]	$\varepsilon_{\sigma_{max}}$ [mm/mm]
0°/90°/45°	43.23	0.03
0°/90°	67.93	0.03
±45°	56.21	0.05

3.4. Impact test

The results of the impact test for samples with different orientations are given in Table 6. The plates with 0°/90° orientation were found to have higher fracture energy than other orientations. Unlike other test results, the orientation that changed the results in the impact test was the presence of 0o/90o orientation, not ±45°. Plates with ±45° orientation have higher fracture energy than plates with 0°/90°/45° orientation. Although the plates with the highest fracture energy were plates with 0°/90° and ±45° orientation, a decrease in fracture energy was observed when these two orientations were combined.

Table 6. Results of glass fiber reinforced composite test plates according to impact tests.

Orientation	Fracture energy [J]
0°/90°/45°	16.8 ± 1.14
0°/90°	18.6 ± 1.76
±45°	17.60 ± 1.60

3.5. Statistical analysis of results

Weibull distributions of the tensile, compression, flexural and impact tests shown in Figure 2 were produced in order to interpret the reliability of the results obtained from 10 repeated tests performed for each plate with ± 45°, 0°/90° and 0°/90°/45° orientations. Weibull parameters and characteristic strengths of the results are given in Table 7. Among the results, for the tensile test, the highest Weibull parameter and characteristic strength were obtained on the plate with 0°/90°, which means that the plate with 0°/90° orientation shows the lower distribution of tensile strength and the plate has a tensile strength of 561.82 with 63.2% probability. For the compression test, although the highest Weibull parameter was obtained on the plate with ± 45° orientation, the highest characteristic strength was obtained on the plate with 0°/90° orientation. In plates with ± 45° orientation shows a lower compressive stress distribution and the plate had a compressive strength of 122.80 MPa with a probability of 63.2%. For the three-point bending test, the highest Weibull parameter and characteristic strength value were seen on the plate with 0°/90°/45° orientation. This means that the plate with 0°/90°/45° orientation shows a lower flexural strength distribution and the plate has a flexural strength of 629.09 MPa with a probability of 63.2%. For the impact test, the highest Weibull parameter and characteristic stress values were obtained from plates with 0°/90°/45° and 0°/90° orientations, respectively.

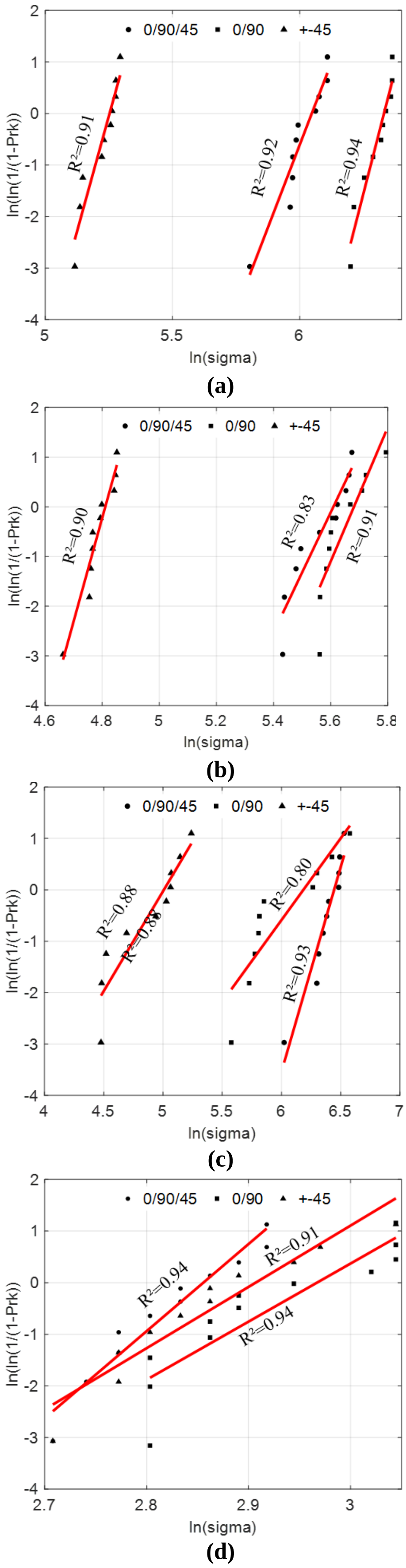

Figure 2. Weibull curves according to plate orientation (a) tensile test (b) compressive test (c) flexural test (d) impact test.

Table 7. Shape factors and characteristic stress values of glass fiber reinforced composite test plates according to tensile tests.

Orientation	Tensile test		Compression test		Three-point bending test		Impact test	
	σ_0 [MPa]	m	σ_0 [MPa]	m	σ_0 [MPa]	m	Fracture energy [J]	m
0º/90º/45º	423.00	12.83	273.04	12.08	629.09	7.96	17.39	16.88
0º/90º	561.82	19.23	293.45	13.50	485.26	3.18	19.44	11.25
±45º	191.04	17.89	122.80	20.79	149.51	3.88	18.30	11.87

Table 8. Average of tensile, three-point bending, compression and impact test results of plates with different orientations.

Orientation	Tensile test		Three-point bending		Compression test		Impact test
	σ [MPa]	ε [%]	σ [MPa]	E [%]	σ [MPa]	ε [%]	energy [J]
0º/90º/45º	406.73	6.02	592.49	3.10	264.40	47.79	17.60
0º/90º	546.89	6.75	431.46	2.70	284.00	41.70	18.60
45º	185.60	23.31	134.70	5.20	118.97	97.00	16.77

It shows that in the Weibull distributions obtained as a result of the experiments, 63% of the maximum strength will be obtained at the point where the graphs cut 0 on the y-axis. Again, the high values of the Weibull parameter obtained from the experimental results mean that the reliability of the experiments performed is high.

According to the Weibull distribution of the tensile and compression tests given in Figure 2a and Figure 2b, the value of the plates with 0°/90° and ±45° orientations cut 0 on the y-axis were highest. Besides, the highest Weibull parameters obtained for the tensile and compression test that was given in Table 3 were observed on the plate 0°/90° and ±45° orientations, respectively.

As shown in Figure 2c, according to the three-point bending test results, the value of the plate with 0°/90°/45° orientation cut 0 on the y-axis was highest and the highest Weibull parameter value was obtained on the plate with the same orientation.

When the impact test Weibull distribution was examined, it was seen in Figure 2d, the curve of the plate with 0°/90° orientation cut 0 at the highest value in the y-axis. On the other hand, the highest Weibull parameter appeared in the plate with ±45° orientation.

4. Conclusions

As seen in Table 8, the tensile and compression test results of the plate with ±45° orientation are similar to the tensile and compression curve of thermoplastic composites under glass transition temperature, respectively. In the plate with 0°/90° orientation, higher tensile and compression strength values were obtained because the glass fibers with 0o orientation bear the load in the pull direction. In the plate with 0°/90°/45° orientation, the glass fiber density with 0o orientation is reduced by including glass fibers with ±45° orientation in the composite. As a result of this, although a decrease in tensile and compression strength was observed, an increase in fiber ratio caused the material to show a linear brittle material behavior.

The plate with ±45° orientation had the highest strain to failure, although it has the lowest bending strength as a result of the three-point bending test. The stress-strain curve of the plates with the orientations 0°/90° and 0°/90°/45° for three-point bending were similar. According to these results, the plate with 0o/90o orientation has the highest flexural strength. Also, the results showed that glass fibers with ±45o orientation added to the composite reduce the bending strength of the composite. The most reliable results and the maximum probability of achieving maximum strength according to the Weibull distributions and Weibull parameters, it was obtained from plates with 0°/90° orientation in tensile tests, ±45° orientation in compression tests and 0°/90°/45° orientation in three-point bending tests. Other results were scattered. According to the results of the Weibull distribution and Weibull parameter of the impact tests, the most reliable test results were obtained in the plate with 0°/90° orientation, while the plate orientation with the highest probability of obtaining the highest strength was determined as 0°/90°/45°.

Acknowledgments

Authors are grateful to EU Horizon 2020 Program under RECOTRANS project with the Grant Agreement number of 768737. Collaboration of the Recotrans Consortium gratefully acknowledged.

Author contributions

Ali Taner Kuzu: Analysis, Writing - original draft

Elifnur Kosemen: Investigation, Testing, Writing - original draft

Aysu Hande Yucel: Testing, Writing - original draft

Mustafa Bakkal: Supervision, Writing - review & editing

References

1. Kosmann, N., Karsten, J., Schuett, M., Schulte, K., & Fiedler, B., Determining the effect of voids in GFRP on the damage behaviour under compression loading using acoustic emission, Composites Part B: Engineering, **2015**, 70:184-188
2. Bazli, M., Jafari, A., Ashrafi, H., Zhao, X., Bai, Y., & Raman, R.S., Effects of UV radiation, moisture and elevated temperature on mechanical properties of GFRP pultruded profiles. Construction and Building Materials, **2020**, 231:117137
3. Bai, Y., & Keller, T., Delamination and kink-band failure of pultruded GFRP laminates under elevated temperatures and compression. Composite Structures, **2011**, 93(2):843-849
4. Yu, B., Till, V., & Thomas, K., Modeling of thermo-physical properties for FRP composites under elevated and high temperature. Composites Science and Technology, **2007**, 67(15-16):3098-3109
5. Biron, M., Thermoplastics and thermoplastic composites, William Andrew, **2018**

6. Pini, T., Caimmi, F., Briatico-Vangosa, F., Frassine, R., & Rink, M., Fracture initiation and propagation in unidirectional CF composites based on thermoplastic acrylic resins. Engineering Fracture Mechanics, **2017**, 184:51-58
7. Kazemi, M.E., Shanmugam, L., Li, Z., Ma, R., Yang, L., & Yang, J., Low-velocity impact behaviors of a fully thermoplastic composite laminate fabricated with an innovative acrylic resin. Composite Structures, **2020**, 250:112604
8. Bhudolia, S. K., & Joshi, S.C., Low-velocity impact response of carbon fibre composites with novel liquid Methylmethacrylate thermoplastic matrix. Composite Structures, **2018**, 203:696-708
9. Obande, W., Ray, D., & Brádaigh, C.M., Ó., Viscoelastic and drop-weight impact properties of an acrylic-matrix composite and a conventional thermoset composite–A comparative study. Materials Letters, **2019**, 238:38-41
10. Boumbimba, R. M., Coulibaly, M., Khabouchi, A., Kinvi-Dossou, A., Bonfoh, N., & Gerard, P., Glass fibres reinforced acrylic thermoplastic resin-based tri-block copolymers composites: Low velocity impact response at various temperatures. Composite Structures, **2017**, 160:939-951
11. Kinvi-Dossou, G., Boumbimba, R. M., Bonfoh, N., Koutsawa, Y., Eccli, D., & Gerard, P., A numerical homogenization of E-glass/acrylic woven composite laminates: Application to low velocity impact. Composite Structures, **2018**, 200:540-554
12. Bhudolia, S. K., Perrotey, P., & Joshi, S.C., Mode I fracture toughness and fractographic investigation of carbon fibre composites with liquid Methylmethacrylate thermoplastic matrix. Composites Part B: Engineering, **2018**, 134:246-253
13. Kinvi-Dossou, G., Boumbimba, R.M., Bonfoh, N., Garzon-Hernandez, S., Garcia-Gonzalez, D., Gerard, P., Arias, A., Innovative acrylic thermoplastic composites versus conventional composites: Improving the impact performances. Composite Structures. **2019**, 217:1-3
14. Kazemi, M.E., Shanmugam, L., Lu, D., Wang, X., Wang, B,, Yang, J., Mechanical properties and failure modes of hybrid fiber reinforced polymer composites with a novel liquid thermoplastic resin, Elium®. Composites Part A: Applied Science and Manufacturing. **2019**, 125:105523
15. Obande, W., Mamalis, D., Ray, D., Yang, L., Brádaigh, C.M., Mechanical and thermomechanical characterisation of vacuum-infused thermoplastic-and thermoset-based composites. Materials & Design, **2019**, 175:107828
16. Cousins, D.S., Advanced thermoplastic composites for wind turbine blade manufacturing. Colorado School of Mines, **2018**
17. Teimouri, M., Hoseini, S. M., & Nadarajah, S., Comparison of estimation methods for the Weibull distribution. Statistics, **2013**, 47(1):93-109